

## PAPER



Cite this: *Soft Matter*, 2016,  
12, 3589

## Hysteretic memory in pH-response of water contact angle on poly(acrylic acid) brushes†

Vivek Yadav, Adrienne V. Harkin, Megan L. Robertson\* and Jacinta C. Conrad\*

We investigated the pH-dependent response of flat polyacid brushes of varying length and dispersity in the extended brush regime. Our model system consisted of poly(acrylic acid) brushes, which change from hydrophobic and neutral at low pH to hydrophilic and negatively charged at high pH, synthesized on silicon substrates using a grafting-from approach at constant grafting density. We observed three trends in the pH-response: first, the dry brush thickness increased as the pH was increased for brushes above a critical length, and this effect was magnified as the dispersity increased; second, the water contact angle measured at low pH was larger for brushes of greater dispersity; and third, brushes of sufficient dispersity exhibited hysteretic memory behavior in the pH-dependence of the contact angle, in which the contact angle upon increasing and decreasing pH differed. As a consequence, the  $pK_a$  of the brushes measured upon increasing pH was consistently higher than that measured upon decreasing pH. The observed pH response is consistent with proposed changes in the conformation and charge distribution of the polyelectrolyte brushes that depend on the direction of pH change and the dispersity of the brushes.

Received 29th December 2015,  
Accepted 7th March 2016

DOI: 10.1039/c5sm03134f

www.rsc.org/softmatter

### Introduction

Stimuli-responsive polyelectrolyte brushes are smart surfaces appropriate for applications in antifouling coatings, sensors, diagnostics, and drug delivery vehicles.<sup>1–3</sup> Annealed polyacid brushes exhibit hydrophilic behavior at high pH (for which the brush is swollen and dissociated) and hydrophobic behavior at

low pH (for which the brush is collapsed and protonated). Annealed polybasic brushes exhibit comparable behavior, with the collapsed state present at high pH and the swollen state present at low pH. The chain conformation, brush height, charge distribution, degree of ionization, and wetting properties of responsive polyelectrolyte brushes depend strongly on the grafting density, salt concentration, and pH of the solution. For example, polyacid brushes at low pH are fully protonated and adopt a conformation similar to that of neutral brushes.<sup>4–7</sup> At high pH, the acid groups on the brush become dissociated and the brush behaves as an extended polyelectrolyte brush in the osmotic or Pincus regime, with a Gaussian density profile.<sup>6–13</sup> At all pH values, the brush density is greatest near the substrate.<sup>7,14–16</sup> The charge density increases with distance from the substrate, and also depends on pH, salt concentration, and grafting density.<sup>15–24</sup> The brush thickness is closely related to the degree of ionization of the brush and resulting polymer conformation, as well as the grafting density.<sup>6,15,18,19,25–28</sup> Despite the existing depth of knowledge on polyelectrolyte brush physics, an improved fundamental understanding of the effects of solution conditions on the brush response is required to design responsive brushes for practical applications. Specifically, open questions remain regarding the mechanism of the brush response to variations in the solution pH, including changes in polymer conformation, degree of dissociation, and charge distribution through the brush.

The simplest method commonly used to probe the degree of dissociation of weak polyelectrolyte brushes is the measurement

*Department of Chemical and Biomolecular Engineering, University of Houston, Houston, TX 77204-4004, USA. E-mail: mrobertson@uh.edu, jconrad@uh.edu*

† Electronic supplementary information (ESI) available: XPS spectrum obtained from an initiator-grafted substrate (Fig. S1); FTIR spectra obtained from PtBA and PAA on the silicon substrate (Fig. S2); <sup>1</sup>H-NMR spectrum obtained from PtBA polymerized in solution (Fig. S3); GPC data obtained from PtBA polymerized in solution (Fig. S4) and resulting  $M_n$  and  $D$  of all polymers (Table S1); as-synthesized dry thickness of all PtBA and PAA brushes reported in this study (Table S1); reduction in PtBA brush thickness upon hydrolysis to PAA (Table S1); camera images of PtBA brushes on silicon substrates (Fig. S5); optical micrographs of PtBA brushes and corresponding PAA brushes (after hydrolysis) (Fig. S6); contact angle as a function of pH for a PAA brush in which the choice of buffered or unbuffered solution for soaking the brush, and the choice of DI water, buffered solution, or unbuffered solution for the contact angle measurement, were varied (Fig. S7) and associated  $pK_a$  values of each curve (Table S2); sigmoidal function fit to  $-\cos(\text{contact angle})$  as a function of pH used to determine the  $pK_a$  in the varying length series (Fig. S8 and S9); pH-dependent contact angle and  $pK_a$  as a function of PAA brush dry thickness (as-synthesized) for brushes grafted from glass substrates (Fig. S10 and Table S3); sigmoidal function fit to  $-\cos(\text{contact angle})$  as a function of pH used to determine the  $pK_a$  in the constant length series (Fig. S11); reversible cycling of thin and thick brushes through pH extrema (Fig. S12); AFM images and root-mean-square surface roughness of PAA brushes (Fig. S13); AFM image showing thickness of PAA brushes (Fig. S14); and dependence of the PAA contact angle on soaking time in solutions of varying pH (Table S4). See DOI: 10.1039/c5sm03134f

of the water contact angle on the brush surface.<sup>29,30</sup> Indeed, the pH-response of the water contact angle for one model polyacid brush, poly(acrylic acid) (PAA), has been measured for brushes of varying grafting densities and lengths.<sup>31–35</sup> Dong *et al.* identified differences between the bulk  $pK_a$  (examined through Fourier Transform Infrared Spectroscopy) and the surface  $pK_a$  (examined through contact angle measurements).<sup>33</sup> They concluded that the acid groups near the substrate are more difficult to ionize and hence have a higher  $pK_a$ .<sup>33</sup> This finding is in agreement with theoretical predictions for weak polyelectrolyte brushes, which indicate that the fraction of charged groups increases with distance from the substrate.<sup>16,18,22,23,36</sup> Other polyelectrolyte brush systems (*e.g.* poly(2-dimethylamino)ethyl acrylate (PDMAEA)) also exhibit differences in the contact angle at low and high pH and between the bulk and surface  $pK_a$  values.<sup>37–39</sup> The difference between bulk and surface  $pK_a$  arises because polyelectrolytes are able to locally regulate the degree of dissociation based on the local dielectric function.<sup>36,40</sup>

By contrast, relatively few literature studies have investigated the pH-response of weak polyelectrolyte brushes when the direction of pH change is varied (*i.e.* upon decreasing or increasing pH). Aulich *et al.* reported hysteresis (which they termed a “memory effect”) in the pH-response of the contact angle of PAA: the  $pK_a$  measured upon increasing pH was significantly larger than that measured upon decreasing pH.<sup>34</sup> This behavior was corroborated with direct measurements of the carboxylic acid and carboxylate anion concentrations at various pH conditions.<sup>34</sup> In polybasic brushes, Wanless and collaborators reported the hysteretic pH-response of the hydrated brush thickness and swelling ratio.<sup>41,42</sup> Finally, Zhulina, Borisov, and Priamitsyn theoretically predicted a hysteresis loop in the grafting density-dependence of various polyelectrolyte brush properties, including the degree of dissociation, brush height, electrostatic potential profile, and polymer and end-segment density profiles.<sup>43</sup> These studies all posit that differences in the location of dissociated charges upon increasing or decreasing pH generate the observed hysteretic memory behavior; the formation of a neutral hydrophobic skin<sup>42</sup> or the charge distribution in the brush<sup>34</sup> may interfere with counterions and/or solvent moving into the brush. These proposed mechanisms involve hindered transport, suggesting that the brush characteristics such as length or dispersity that influence ion movement into or out of the brush may be critical parameters governing the extent of hysteretic memory behavior.

The effects of brush length and dispersity on the pH-response of weak polyelectrolyte brushes, surprisingly, have not been systematically explored. Previous studies on poly(methacrylic acid) (PMAA) brushes reported length-independent  $pK_a$  values over a wide range of brush lengths.<sup>44,45</sup> In both studies, the effect of the direction of pH change was not characterized. In polybasic brushes, the dry brush thickness was reported to significantly affect the hysteretic pH-response of the hydrated brush thickness and swelling ratio,<sup>41,42</sup> the pH-response of the degree of dissociation, however, was not explored. To our knowledge, the effect of dispersity (in the molecular weight distribution) on the brush pH-response has not been directly explored in the literature. Systematic studies of the effect of

brush length and dispersity on pH-response are expected to generate insight into the physical mechanisms underlying charge dissociation and hysteretic memory.

Here, we characterize the effect of the direction of pH change on the response of the water contact angle and dry thickness of model weak polyacid brushes of varying length and dispersity. PAA brushes of as-synthesized dry thicknesses in the range of 7–44 nm were synthesized through surface-initiated atom transfer radical polymerization (SI-ATRP) of *tert*-butyl acrylate, followed by hydrolysis to PAA. Dry brush thickness (*via* ellipsometry) and water contact angle were measured after brushes were exposed to solutions of varying pH. The brushes were first exposed to solutions of decreasing pH (from 10 to 3), and subsequently exposed to solutions of increasing pH (from 3 to 10). We report three trends in the response of the PAA brushes to changes in pH. First, the thickness of dry brushes increased as the pH was increased for brushes above a critical length, and this effect was magnified as the dispersity increased. Second, the water contact angle measured at low pH increased with brush dispersity. Finally, brushes of sufficiently high dispersity exhibited hysteretic memory behavior (*i.e.* dependent on the direction of pH change) in the contact angle. We propose a mechanism to relate the observed pH response of PAA brushes in this study to behavior reported in the literature for the polymer conformation, charge distribution, and degree of penetration of solution throughout the brushes, and show that an increase in brush dispersity generates the hysteretic memory behavior.

## Materials and methods

### Materials

All chemicals were purchased from Sigma Aldrich and used as-received unless otherwise noted. Monomethyl ether hydroquinone (inhibitor) was removed from *tert*-butyl acrylate (*t*BA, 98%) by passing through a silica gel column (60 Å pore size). *t*BA was then dried with calcium hydride (reagent grade, 95%) and distilled under vacuum. Ethyl  $\alpha$ -bromoisobutyrate (EBiB, 98%) and  $N,N,N',N',N''$ -pentamethyldiethylenetriamine (PMDETA, 99%) were each degassed with three freeze–pump–thaw cycles. Dichloromethane (JT Baker, HPLC grade, 99.8%) was dried using a Pure Process Technology solvent purification system.

### Immobilization of initiator on silicon wafer

Initiator attachment to silicon substrates followed procedures in ref. 46. Single-sided polished silicon wafers (Mechanical Grade, University Wafers) were cut into approximately 1 cm  $\times$  2 cm pieces before use. The silicon substrates were cleaned by 10 min of sonication in acetone (ACS reagent, 99.5%) followed by 10 min of sonication in deionized (DI) water. After drying under nitrogen, the wafers were exposed to air plasma (Harrick Plasma Cleaner) for three minutes to generate surface hydroxyl groups. (3-Aminopropyl)triethoxysilane (APTES, 99%) was deposited on the wafer in vacuum for 30 min at a vacuum level of 50 mtorr. The silanized surface on the silicon substrate was annealed at 110 °C for 30 min. Subsequently, the silicon substrate was

immersed in dry dichloromethane containing 2 vol% anhydrous pyridine (99.8% pure). The polymerization initiator,  $\alpha$ -bromoisobutryl bromide (98%), was added dropwise into the solution containing the substrate at 0 °C until an initiator concentration of 0.081 M was attained. The resulting solution was held at 0 °C for 1 hour and then at room temperature for 12 hours. The initiator-grafted substrate was rinsed with acetone and dried under flow of nitrogen gas. The silicon substrates grafted with initiator were used immediately for polymerization.

### Synthesis of poly(acrylic acid) (PAA) brushes

Poly(*tert*-butyl acrylate) (PtBA) brushes were synthesized using surface-initiated atom transfer radical polymerization (SI-ATRP) and subsequently hydrolyzed to PAA (Scheme 1), following procedures in ref. 47 and 48. The initiator-grafted silicon substrates were transferred to a glove box under nitrogen gas in a round bottom flask where *t*BA, PMDETA, copper(i) bromide (CuBr, 99%), anhydrous *N,N*-dimethylformamide (DMF, 99.8%), and EBiB (a solution initiator) were added in a predetermined molar ratio for each polymerization. The flask was capped with a septum inside the glove box and transferred to a preheated oil bath at 50 °C. The reaction mixture was stirred for 24 hours and [tBA]:[EBiB] was varied to obtain different PtBA brush lengths. An equimolar ratio of PMDETA, EBiB, and CuBr was used, and this mixture was diluted with DMF such that the volume ratio of DMF : *t*BA was 1 : 1.

The polymerization was quenched by addition of tetrahydrofuran (THF, OmniSolv, HPLC grade, 99.9%). The silicon substrate grafted with PtBA was rinsed with acetone, methanol (ACS reagent, 99.8%), and DI water, and dried under nitrogen gas. The PtBA brushes were stored in a petri dish. The PtBA brush was converted to a PAA brush by hydrolysis in the presence of dichloromethane (11 ml) and trifluoroacetic acid (reagent plus, 99%, 3 ml) for 24 hours. The PAA brush on a silicon substrate was rinsed with acetone and dried under nitrogen flow.

The remaining solution, which contained free PtBA (initiated from EBiB), was diluted by adding excess THF and passed through a neutral aluminum oxide column to remove the catalyst. The polymer solution devoid of catalyst was concentrated using a rotary evaporator and precipitated in a DI water/methanol mixture

(1 : 1 by volume). Finally, the precipitated PtBA was collected and dried under vacuum overnight at room temperature.

Two separate methods were employed to synthesize brushes of constant length and varying dispersity. In one synthesis, the procedure described above was modified to use a higher ratio of initiator (EBiB) to catalyst (CuBr) and ligand (PMDETA) (20 : 1 : 1) and a longer reaction time of 32 hours, resulting in a PtBA brush of length 6.3 nm and dispersity 1.26 (methods used to characterize the length and dispersity are discussed in the following sections). In a second reaction, a reducing agent (phenylhydrazine), which is known to decrease the concentration of Cu<sup>II</sup> deactivator,<sup>49</sup> was employed. Phenylhydrazine (97%) was added to the reagents described above (the molar ratio of phenylhydrazine : initiator : catalyst : ligand was 0.5 : 1 : 1 : 1 and the reaction time was 24 h), resulting in a PtBA brush of length 7.3 nm and dispersity 1.54. Both brushes were subsequently hydrolyzed to PAA.

### Gel permeation chromatography (GPC)

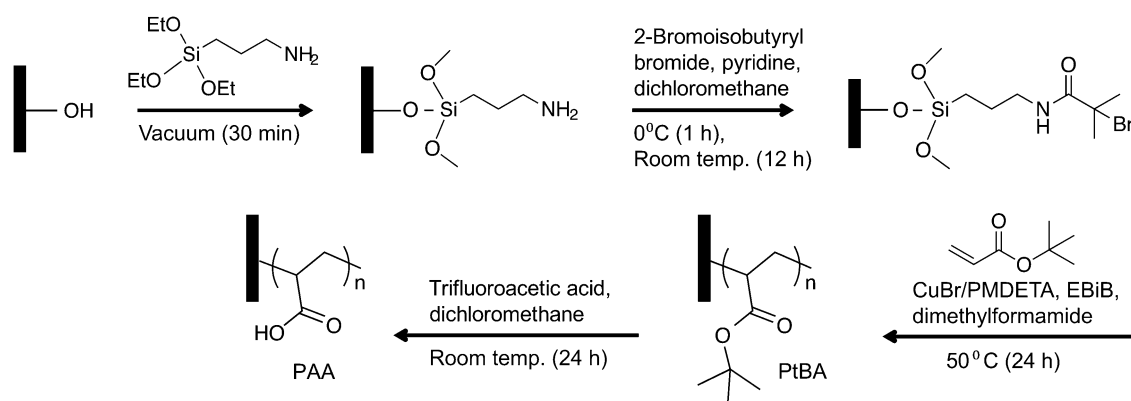
Molecular weight and molecular weight distribution (including the number-average molecular weight,  $M_n$ , and dispersity,  $D$ ) for free polymer (synthesized in solution) were measured with a Viscotek GPC system with Agilent ResiPore columns, using stabilized THF (OmniSolv, HPLC grade, >99.9%) as the mobile phase at 30 °C. The flow rate was 1 ml min<sup>-1</sup> and injection volume was 100  $\mu$ l. A triple detection system, including light scattering, viscometer, and differential refractometer, was used to characterize the molecular weight distribution. The  $dn/dc$  value of PtBA was determined to be  $0.0479 \pm 0.0012$  under these conditions.

### Proton nuclear magnetic resonance (<sup>1</sup>H-NMR)

<sup>1</sup>H-NMR spectra were collected on a JEOL ECA-500 spectrometer using deuterated chloroform as the solvent and tetramethyl silane (TMS) as an internal reference.

### X-ray photoelectron spectroscopy (XPS)

XPS spectra were obtained with a Physical Electronics Model 5700 instrument using a monochromatic Al K $\alpha$  X-ray source (1486.6 eV) operated at 350 W. The diameter of the analyzed



Scheme 1 Synthesis of PAA brushes.

area, the collection solid cone angle, and the take-off angle were fixed at 0.8 mm, 5°, and 45°, respectively. An applied pass energy of 23.5 eV resulted in an energy resolution of better than 0.51 eV. Measurements were conducted at a vacuum level of  $5 \times 10^{-9}$  torr or lower.

### Atomic force microscopy (AFM)

AFM images were acquired with a multimode atomic force microscope (Nanoscope IV) from Digital Instruments operated in tapping mode using monolithic silicon Tap300Al-G probes. The resonance frequency was 300 kHz and force constant was 40 N m<sup>-1</sup>. Images were collected in height and amplitude (or deflection) modes with scan rates between 2–3 s<sup>-1</sup> and 256 scan lines per image.

### Fourier transform infrared spectroscopy (FTIR)

Infrared (IR) absorbance was measured using a Nicolet 6700 FTIR spectrometer equipped with an attenuated total reflectance (ATR) stage. IR absorbance was recorded with OMNIC data acquisition software using 128 scans at a resolution of 8 cm<sup>-1</sup>. IR peak locations were used to characterize PtBA and PAA brushes grafted on silicon wafers.

### Water contact angle and thickness of dried PAA brushes

To investigate the dependence of the water contact angle and dry brush thickness on pH, separate solutions of pH ranging from 3 to 10 were prepared by adding an appropriate amount of sodium hydroxide (ACS reagent, >97%) or hydrochloric acid (Ricca Chemical Company, 1% v/v aqueous solution) to water purified with a Millipore water purification system (resistivity 18.2 MΩ cm). The polymer-grafted silicon wafers were immersed for 30 min in a solution with a desired pH and subsequently dried under nitrogen.

Static water contact angles on the dried PAA brush samples were measured on an OCA 15EC video-based optical contact angle-measuring instrument (DataPhysics, Germany) at ambient temperature using SCA 20 software. DI water droplets (of approximate volume 1 μl) were deposited carefully onto the polymer-grafted surface and the contact angles were measured at five different positions on the surface.

The dry thickness of the PAA brushes was measured with a JA Woollam M-2000 spectroscopic ellipsometer. Ellipsometry data were modeled using a two-layer model that consisted of a polymer layer on top of SiO<sub>2</sub>. The wavelength (λ) dependence of the refractive index (n) of each layer was modeled with the Cauchy dispersion relation,  $n(\lambda) = A + B/\lambda^2$  (A and B are strictly positive). The measured amplitude ratio and phase difference were modeled with the Fresnel equation, with the brush thickness as a fitting parameter. This model provided a good fit for data in the wavelength range of 350–1690 nm. Thickness measurements were conducted at five different locations on each substrate.

## Results

### Brush synthesis

PtBA brushes of varying length on silicon wafers were synthesized using SI-ATRP, as shown in Scheme 1. The attachment of

APTES and SI-ATRP initiator to the silicon substrate was verified through XPS (Fig. S1 in the ESI†).<sup>48</sup> The presence of the PtBA brush was confirmed through FTIR (Fig. S2 in the ESI†).<sup>6,7,27,33,47,50–53</sup> In the first series of experiments (hereafter, series 1), we synthesized brushes of varying length and dispersity by varying the amount of monomer in solution. To estimate the grafting density of brushes on the substrate, we examined the relationship between the as-synthesized dry thickness of the PtBA brush, measured using ellipsometry, and the  $M_n$  of PtBA. As the  $M_n$  of PtBA grafted to the substrate could not be directly characterized, a solution initiator (EBiB) was added to every brush synthesis. The solution PtBA was characterized through <sup>1</sup>H-NMR (Fig. S3 in the ESI†)<sup>54–57</sup> and GPC (Fig. S4 and Table S1 in the ESI†). The PtBA dry brush thickness appeared to be uniform across the substrate (Fig. S5 and S6 in the ESI†) and increased linearly with  $M_n$  of the solution PtBA (Fig. 1), consistent with a constant brush grafting density. We estimated the grafting density of the PtBA brushes as  $\sigma = h\rho N_A/M_n$ ,<sup>27</sup> where  $h$  is the brush thickness,  $\rho = 1.05$  g cm<sup>-3</sup> is the density of PtBA,<sup>27</sup>  $N_A$  is Avogadro's number, and  $M_n$  is the molecular weight of the solution polymer, which is assumed to be equal to that of the brush (following prior studies<sup>6,27,47</sup>). Although the  $M_n$  of the solution polymer was likely not equal to that of the brush and water from humid air adsorbed into the brush may have increased the height by up to 30%,<sup>40</sup> the linear scaling of the solution polymer  $M_n$  with brush thickness nonetheless suggested that the grafting density was constant for all brushes. From the linear scaling of  $M_n$  with brush thickness, we estimated a grafting density of 0.38 chains per nm<sup>2</sup> for all brushes described in this manuscript (unless otherwise indicated). For PtBA brushes of a lower molecular weight ( $M_n = 8.56$  kg mol<sup>-1</sup>), the crossover from the mushroom to brush regime occurred at 0.08 chains per nm<sup>2</sup> [ref. 27]. We therefore assumed that all brushes in this study were in the (extended) brush regime, even after accounting for errors in the brush thickness due to atmospheric water taken up by the brush.

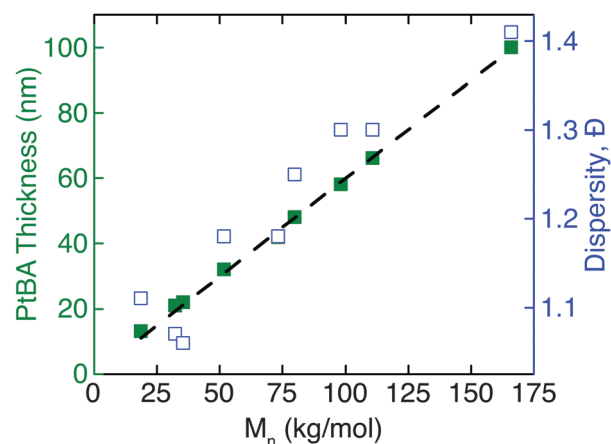


Fig. 1 PtBA brush dry thickness (as-synthesized, closed symbols, left y-axis) and dispersity ( $D$ , open symbols, right y-axis) as a function of molecular weight ( $M_n$ ) of PtBA solution polymer. The error bars on each measurement are smaller than the symbols and represent the standard deviation in measurements obtained from the same substrate. The dashed line indicates a linear fit ( $R^2 = 0.99$ ) to the thickness versus  $M_n$  data.

We also measured the dispersity ( $\mathcal{D}$ ) of the solution polymer that was co-polymerized during brush synthesis. Here we explicitly assumed that the dispersity of the solution polymer is proportional to that of the polymer brush on the surface; this assumption is analogous to that frequently used to estimate the molecular weight of surface-grafted polyelectrolyte brushes,<sup>27</sup> in which the molecular weight of the solution polymer is assumed to be proportional to that of the brush. The dispersity ( $\mathcal{D}$ ) of the solution polymer was relatively low, 1.1–1.2, over a wide range of  $M_n$  (18.6–73.3 kg mol<sup>-1</sup>), as shown in Fig. 1 and in Fig. S4 and Table S1 in the ESI.† At higher  $M_n$  the molecular weight distribution was broader, with  $\mathcal{D} \sim 1.3$ –1.4 for  $M_n$  of 79.9–167 kg mol<sup>-1</sup>.

PtBA brushes on silicon wafers were subsequently hydrolyzed to PAA for characterization of the pH-dependent response. FTIR spectroscopy (Fig. S2 in the ESI†) showed the disappearance of the absorbance maxima at 2977 and 1392/1368 cm<sup>-1</sup>, associated with asymmetric stretching and bending of the *tert*-butyl methyl group of PtBA, and appearance of the absorbance maximum at 3420 cm<sup>-1</sup>, associated with OH stretching of PAA, confirming that PtBA was successfully converted to PAA.<sup>6,27,47,58–60</sup> After hydrolysis, the decrease in the thickness of the brushes, measured with ellipsometry as 48–56% (Table S1 in the ESI†), was also consistent with the expected decrease in the volume of the polymer.<sup>27</sup>

### pH response of PAA brushes of varying length and dispersity (series 1)

PAA brushes were immersed in unbuffered solutions of constant pH for 30 minutes to allow sufficient time for swelling or deswelling. Subsequently, we measured the brush thickness (using ellipsometry) and the static contact angle<sup>29,30</sup> of a neutral (pH 7) water droplet<sup>46,61</sup> on the brush surface; we use the latter method as a simple and rapid way to assess the degree of dissociation within the brush. We confirmed that the thickness and static contact angle did not change on time scales longer than 30 minutes for unit increment changes in pH. Additionally, we confirmed that the choice of a phosphate-buffered or unbuffered soaking solution, and the choice of DI water, phosphate-buffered solution at a given pH, or unbuffered solution at a given pH used as the droplet for the contact angle measurement, did not affect the measured contact angle (Fig. S7 and Table S2 in the ESI†); this finding is in agreement with earlier measurements showing that buffer negligibly affected the water contact angle on brushes.<sup>35</sup> Finally, we limited our measurements to a pH range of 3–10 because brushes exposed to solutions of pH 2 did not exhibit reproducible changes upon cycling pH; we attributed this non-reproducibility to cleavage of the polymer chains by hydrolysis of the ester bonds.<sup>33</sup>

In the series 1 experiments, the dry thickness of a short 12 nm brush decreased slightly upon decreasing pH from 10 to 3 (Fig. 2(a)). Longer brushes (*e.g.* 22, 30, and 44 nm) exhibited a more pronounced decrease in thickness as pH was decreased. The decrease in thickness with decreasing pH reported here is consistent with prior measurements on flat brushes.<sup>21,59</sup> The thickness did not depend on the direction of pH change (increasing or decreasing) for brushes of thickness 12, 22,

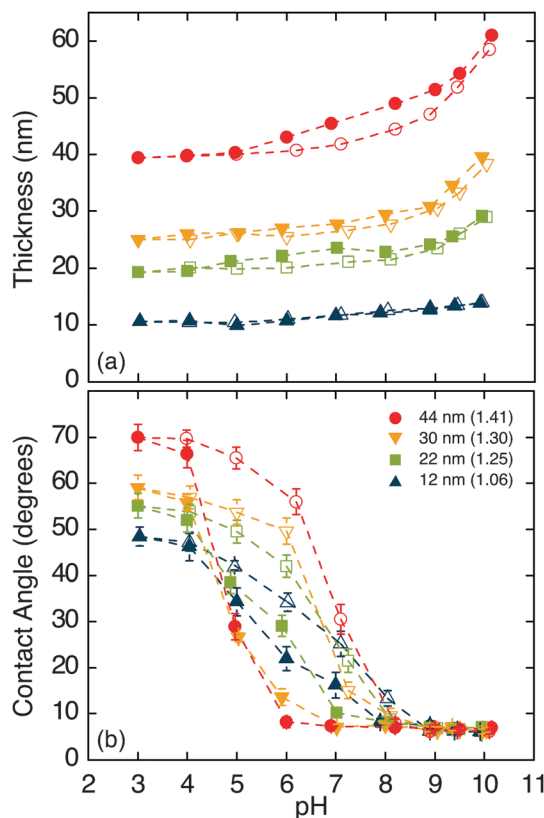


Fig. 2 (a) Dry thickness and (b) static water contact angle of PAA brushes of varying length and dispersity (series 1), as a function of pH. The pH was first decreased from 10 to 3 (closed symbols) and then increased from 3 to 10 (open symbols). Symbols indicate the as-synthesized dry thickness (dispersity,  $\mathcal{D}$ ) of each brush: blue  $\blacktriangle$ : 12 nm (1.06); green  $\blacksquare$ : 22 nm (1.25); orange  $\blacktriangledown$ : 30 nm (1.30); and red  $\bullet$ : 44 nm (1.41). The contact angle measurements exhibit significant hysteric memory, in contrast to the behavior of the dry thickness. Error bars represent the standard deviation from at least five measurements obtained from the same substrate; the error bars on the dry thickness measurements in (a) are smaller than the symbols.

and 30 nm. Only the thickest brush (44 nm) exhibited a slight hysteresis in the thickness response, with the dry thickness upon decreasing pH slightly larger than that upon increasing pH. To quantify the change in dry thickness we calculated the percentage increase in the dry thicknesses from pH 3 to 10 (Table 1). The percentage increase in thickness was approximately constant save for the thinnest brush.

The contact angle of neutral water on a PAA brush after immersion in a solution of pH 10 was low ( $<10^\circ$ ) and characteristic of a hydrophilic surface (Fig. 2(b)), independent of brush length. The low contact angle is consistent with the ionization of the great majority of the acrylic acid groups.<sup>34,62</sup> For a brush of as-synthesized dry thickness 12 nm, the water contact angle increased to 48 degrees as the pH was decreased from 10 to 3, consistent with protonation of the acrylic acid groups. The contact angle at low pH increased with increasing brush length and dispersity, reaching 70 degrees for a brush of as-synthesized dry thickness 44 nm and dispersity 1.41.<sup>33</sup>

Upon increasing the pH from 3 to 10, the contact angle on all brushes decreased and the brushes returned to the deprotonated

**Table 1** Percentage increase in dry thickness of PAA brushes (series 1, varying length and dispersity), measured as pH is increased from 3 to 10

As-synthesized dry thickness (nm)	Dispersity, $D$	Percentage increase in dry thickness <sup>a</sup>
11.7 ± 0.3	1.06	30 ± 5
22.2 ± 0.8	1.25	51 ± 5
30.4 ± 0.4	1.30	58 ± 4
44.2 ± 0.3	1.41	55 ± 2

<sup>a</sup> Percentage increase in dry thickness = 100 [(dry thickness at pH 10) – (dry thickness at pH 3)]/(dry thickness at pH 3); standard deviation was calculated using measurements obtained from the same substrate.

and hydrophilic state at high pH. Notably, the water contact angles measured upon increasing and decreasing pH differed over an intermediate pH range of 5–8. This hysteretic memory behavior was observed over a wide range of brush lengths and dispersities (Fig. 2(b)). Our findings confirm and significantly extend an earlier report of hysteresis by Aulich *et al.*, who observed similar differences in the contact angle (which they termed a “memory effect”) measured for a brush of dry thickness ~5 nm cycled between pH 2 and 10; the brush dispersity was not reported.<sup>34</sup>

Motivated by this hysteretic change in contact angle with pH, we examined the behavior of the logarithm of the effective acid dissociation constant,  $pK_a$ , defined as the midpoint of the contact angle titration curve; knowledge of  $pK_a$  is important to accurately gauge brush response in practical settings. We fit the cosine of the contact angle profile, which is related to the degree of dissociation of the carboxylic groups near the free surface of the brush,<sup>29,30</sup> to a sigmoidal function. From the fit, we extracted  $pK_a$  upon increasing and upon decreasing pH (Fig. S8 and S9 in the ESI†); this calculation relies on the assumption that the change in the liquid–solid interfacial energy is linearly proportional to the fraction of ionized groups.<sup>29</sup> PAA brushes exhibited distinct differences in  $pK_a$  upon increasing and decreasing pH (Fig. 3). The  $pK_a$  measured upon increasing pH for a given brush length and dispersity was always greater than that measured upon decreasing pH, in agreement with prior work on a single brush length.<sup>34</sup> Upon increasing pH, the measured  $pK_a$  (6.1–6.5) was comparable to that previously reported for PAA in solution (6.2)<sup>63</sup> and a “bulk”  $pK_a$  of thick 55 nm PAA brushes measured by FTIR titration (6.5–6.6).<sup>33</sup> By contrast, the  $pK_a$  values measured upon decreasing pH (4.6–5.0) were similar to the previously reported “surface”  $pK_a$  of the 55 nm PAA brushes (4.4)<sup>33</sup> and 12 nm brushes (4.8)<sup>35</sup> measured *via* contact angle titration.<sup>37</sup> We observed similar direction-dependent  $pK_a$  values for brushes polymerized on glass coverslips (Fig. S10 in the ESI†).

Two earlier studies examined the length-dependence of  $pK_a$  in poly(methacrylic acid) (PMAA) brushes. Schüwer and Klok measured the frequency-dependent response using quartz crystal microbalance (QCM) and found that the  $pK_a$  of PMAA (measured upon increasing pH) was constant as the brush length increased from 5 nm to 80 nm (with a slight increase in  $pK_a$  for a brush of length 91 nm),<sup>45</sup> and Santonicola *et al.* reported that PMAA brushes of length ~30 nm and ~90 nm

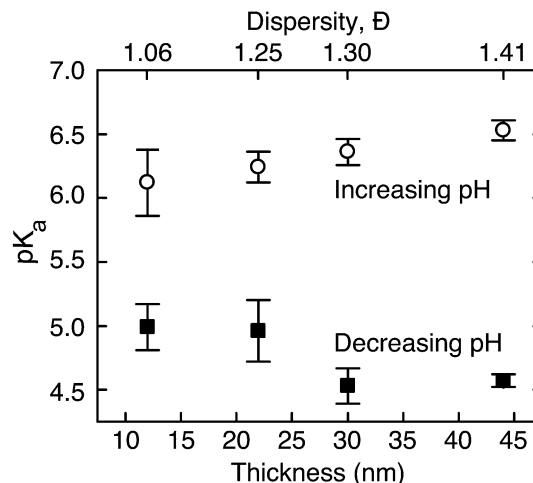


**Fig. 3** Logarithm of the acid dissociation constant,  $pK_a$ , as a function of PAA brush dry thickness (as-synthesized) in series 1 (varying length and dispersity). The closed (open) symbols indicate  $pK_a$  values calculated from contact angle curves measured as the pH is decreased (increased). The upper x-axis labels indicate the dispersity of each brush. Error bars were extracted through the fit to the sigmoidal curve.

exhibited similar  $pK_a$  values.<sup>44</sup> In both studies, the relative insensitivity of the  $pK_a$  to the PMAA brush length is in agreement with our results (Fig. 3) for PAA brushes of lengths 12–44 nm; neither study reported the brush dispersity.

### Decoupling effects of brush thickness and dispersity (series 2)

To directly test the effects of dispersity on brush response, in a second series of experiments (series 2) we synthesized three PAA brushes of similar length but varying dispersity. Using an equimolar (1 : 1 : 1) ratio of initiator (EBiB) to catalyst (CuBr) and ligand (PMDTA), we obtained a PtBA brush of length 13.4 nm and dispersity  $D$  of 1.11; using a higher ratio of initiator to catalyst and ligand of 20 : 1 : 1, we obtained a PtBA brush of length 12.7 nm and dispersity  $D$  of 1.26. Lastly, we produced a PtBA brush of similar length (14.4 nm) and even greater dispersity  $D$  (1.54) by adding a reducing agent, phenylhydrazine. All three brushes were hydrolyzed to PAA. The thickness of PAA brushes produced through these three different synthetic methods were comparable and did not vary with pH, (Fig. 4(a) and Table 2). The contact angle of the lowest-dispersity PAA brush ( $D = 1.11$ ) exhibited no measurable hysteretic memory upon reversing the direction of pH change, whereas the contact angle of both higher-dispersity brushes ( $D = 1.26$  and 1.54) exhibited significant hysteretic memory. Furthermore, the low-pH static contact angles of the two higher-dispersity brushes were indistinguishable from one another, yet significantly larger than that of the lowest dispersity brush. The similarity of the low-pH contact angles for the two higher-dispersity brushes suggests that there may be an upper limit to the enhancement in the low-pH contact angle in the limit of high dispersity values; this result contrasts with that found in series 1 experiments (varying length and dispersity), in which the low-pH contact angle systematically increased with dispersity (Fig. 2(b)).

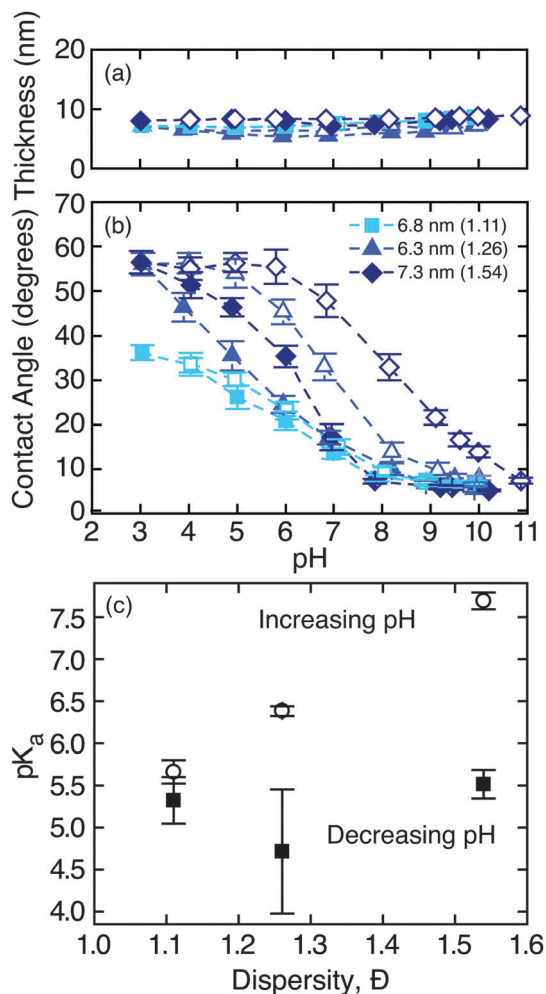


**Fig. 4** (a) Dry thickness and (b) static water contact angle as a function of pH for PAA brushes of fixed length ( $\sim 7$  nm) and varying dispersity (series 2). The pH was first decreased from 10 to 3 (closed symbols) and then increased from 3 to 10 (open symbols). Symbols in (a) and (b) indicate the as-synthesized dry thickness (dispersity,  $D$ ) of each brush: light blue  $\blacksquare$ : 6.8 nm (1.11); medium blue  $\blacktriangle$ : 6.3 nm (1.26); dark blue  $\blacklozenge$ : 7.3 nm (1.54). In (c), the  $pK_a$  is shown as a function of dispersity  $D$ , measured upon decreasing pH ( $\blacksquare$ ) followed by increasing pH ( $\circ$ ). The higher-dispersity brushes exhibit significant hysteretic memory in contact angle, in sharp contrast to the lack of hysteretic memory observed from the lower-dispersity brush. Error bars in (a) and (b) represent the standard deviation from at least five measurements obtained from the same substrate; the error bars on the dry thickness measurements in (a) are smaller than the symbols. Error bars in (c) represent the maximum value of the standard error resulting from the best fit of the sigmoidal curve to the data in (b).

The  $pK_a$  was characterized as the midpoint of the contact angle titration curves; sigmoidal fits to the data in Fig. 4(b) are shown in Fig. S11 in the ESI.† The  $pK_a$  values measured for the lowest-dispersity brush in Fig. 4(b) upon increasing or upon decreasing pH were identical, as that brush did not exhibit hysteretic memory behavior. Brushes of higher dispersity exhibited differences in the  $pK_a$  values measured upon decreasing and increasing pH. The  $pK_a$  values obtained upon decreasing pH were approximately independent of brush dispersity (closed symbols in Fig. 4(c)) and were consistent with those reported in

**Table 2** Percentage increase in dry thickness of PAA brushes of varying dispersity and approximately constant length (series 2), measured as pH is increased from 3 to 10

As-synthesized dry thickness (nm)	Dispersity, $D$	Percentage increase in dry thickness <sup>a</sup>
$6.8 \pm 0.2$	1.11	$20 \pm 5$
$6.3 \pm 0.2$	1.26	$< 1$
$7.3 \pm 0.1$	1.54	$4 \pm 1$

<sup>a</sup> Percentage increase in dry thickness =  $100 [(dry\ thickness\ at\ pH\ 10) - (dry\ thickness\ at\ pH\ 3)] / (dry\ thickness\ at\ pH\ 3)$ ; standard deviation was calculated using measurements obtained from the same substrate.

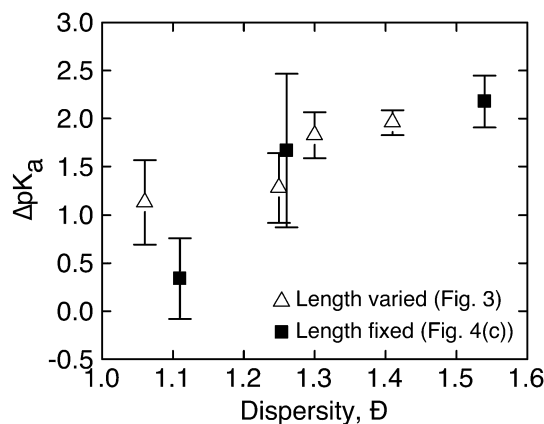


**Fig. 5** Difference in  $pK_a$ ,  $\Delta pK_a = (pK_a, \text{increasing pH}) - (pK_a, \text{decreasing pH})$  as a function of dispersity  $D$  for brushes of varying length (series 1, length = 12–44 nm, extracted from Fig. 3) and brushes of fixed length (series 2, length = 7 nm, extracted from Fig. 4(c)).

Fig. 3 for series 1 brushes (varying length and dispersity). As pH was increased from 3 to 10, however, the  $pK_a$  surprisingly yet systematically increased with dispersity (Fig. 4(c)); by contrast, in series 1 experiments (varying dispersity and length, Fig. 3), the  $pK_a$  observed upon increasing pH was independent of both brush length and dispersity. We defined the difference in  $pK_a$ ,  $\Delta pK_a = (pK_a, \text{increasing pH}) - (pK_a, \text{decreasing pH})$ , and examined its dependence on  $D$  for brushes of varying length (series 1, extracted from Fig. 3) or fixed length (series 2, extracted from Fig. 4(c)). Across all samples,  $\Delta pK_a$  increased with increasing  $D$  (Fig. 5). Because hysteretic memory behavior disappeared as dispersity was decreased, we suggest that dispersity is the dominant factor underlying the hysteretic memory behavior. The dependence of  $\Delta pK_a$  on brush properties is important for applications that require precise control over brush response over multiple switching cycles.

## Discussion

In series 1 experiments (varying length and dispersity), the response of PAA brushes to changes in pH exhibited three trends (Fig. 2 and 3). (i) The dry thickness decreased as the pH was decreased, and the percentage increase in dry thickness was nearly constant for the brushes of greater length and

dispersity (lengths between 22–44 nm and dispersities between 1.25–1.41). (ii) The low-pH contact angle of water on dry brushes following immersion in solution of pH 3 increased with increasing brush length and dispersity. (iii) All brushes exhibited hysteretic memory behavior at intermediate pH, in which the contact angles measured upon increasing and decreasing pH were different. The  $pK_a$  observed upon increasing pH was significantly higher than that observed upon decreasing pH.

Similar but slightly different trends were observed in series 2 experiments (fixed length and varying dispersity, Fig. 4). (i) The dry thickness of these relatively short (7 nm) brushes was independent of dispersity and increased only slightly with pH (Table 2). (ii) The low-pH contact angles of the higher dispersity brushes were comparable to one another, but were significantly higher than that of the low-dispersity brush. (iii) The two higher dispersity brushes exhibited hysteretic memory behavior, whereas the pH-response in the low dispersity brush did not depend on the direction of pH change.

Finally, the difference in  $pK_a$  (characterized upon decreasing and increasing pH) increased slightly with increasing dispersity when both series 1 and 2 were considered together (Fig. 5).

To explain the observed trends in dry thickness and contact angle we consider the effect of changing pH on the dissociation of the carboxylic acid groups in the brush and on polymer conformation, as reported in earlier literature studies. At pH 3, the acid groups are protonated throughout the brush, and the brush is uncharged and somewhat hydrophobic. Earlier ionic concentration measurements indicated that at pH 3 the solution does not penetrate the brush.<sup>34</sup> The relatively high contact angle of neutral water on the dry brush observed at pH 3 is thus consistent with a hydrophobic brush periphery. As the pH of the solution is increased, the acid groups at the surface start to become deprotonated.<sup>33</sup> Theory and simulations,<sup>16,18,22,23</sup> as well as experiments,<sup>33</sup> indicated that the degree of dissociation in weak polyacid brushes increases as the distance from the substrate is increased. At pH 10, the carboxylic acid groups in the solvent-soaked brushes are mostly deprotonated and the brushes are swollen and extended. The low contact angle indicates that solution fully penetrates the charged, hydrophilic brush; this result is consistent with earlier ionic concentration measurements at high pH.<sup>34</sup> For all brushes, it is possible to cycle the brush between very low and very high pH values (outside of the pH range over which hysteretic memory is observed in Fig. 2), and reversibly recover surfaces with high and low contact angles, respectively (Fig. S12 of the ESI†); this finding indicates that the conformational changes at extreme pH values are reversible.

The hysteretic memory in contact angle observed in our experiments suggests that the polymer conformation affects the ability of solvent and counterions to penetrate the brush at intermediate pH values. Earlier studies suggest that polyelectrolytes can locally regulate the degree of dissociation of the charge groups based on the local dielectric environment.<sup>36,40</sup> We thus propose a hypothesized physical picture similar to those used to describe changes in conformation in polybasic<sup>42</sup> and polyacid<sup>34</sup> brushes upon increasing or decreasing pH,

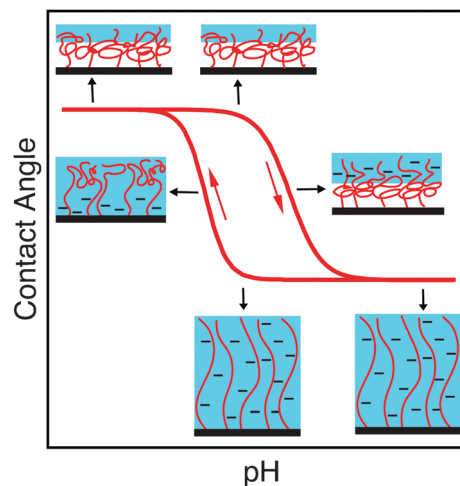


Fig. 6 Proposed mechanism for changes in brush conformation and charge distribution as a function of pH. We hypothesize that the change in thickness and the hysteretic memory in contact angle observed in this study arise from differences in the protonation of the brush at the periphery and interior at intermediate pH upon increasing or decreasing pH. The schematic indicates the proposed hydrated state of the brush.

as shown in Fig. 6. This picture is based on an earlier literature report of hysteresis in dissociation of the carboxylic groups upon changing pH.<sup>34</sup> Upon decreasing the pH from 10, the brush remains water-wet over several pH units. Contact angle is thought to probe the ionization state of the charge groups far from the substrate<sup>33</sup> and so our findings suggest that upon decreasing pH these acid groups remain charged until the pH is lowered significantly below 10. When the pH is sufficiently lowered, the brush begins to collapse as the groups on the periphery become uncharged, leading to an increase in the contact angle.

Conversely, when the pH is increased from 3 to 10 the initial change in contact angle is gradual. This result suggests a delayed onset of deprotonation, with the periphery of the brush remaining hydrophobic and collapsed. A possible explanation for the delayed collapse is suggested by two sets of earlier measurements. First, using the standing X-ray technique Aulich *et al.* showed that ions do not penetrate hydrophobic PAA brushes at low pH.<sup>34</sup> Second, *via* turbidity measurements Sarkar and Somasundaran showed that high molecular weight PAA brushes phase separate from solution at low pH under which intramolecular hydrogen bonding occurs, whereas low molecular weight PAA brushes remain suspended in solution; both enthalpic and entropic contributions to the free energy, and hence the driving force for the phase separation, increase with molecular weight.<sup>64</sup> These earlier results therefore suggest that the delay in the onset of swelling observed in our study, as pH is increased from 3 to 10, arises from the inability of the solvent to interact with collapsed and phase-separated PAA brushes.

We considered several possible origins of the observed trends in the pH-response of the contact angle and dry thickness shown in Fig. 2–4, which are hypothesized to result from underlying changes in PAA brush conformation and charge distribution

shown schematically in Fig. 6. First, we determined that PtBA was fully converted to PAA within measurement error, based on the complete disappearance of characteristic PtBA peaks in the FTIR measurements (Fig. S2, ESI†) and the near-zero CA as observed at high pH. Second, we measured the characteristic roughness of dry brushes using atomic force microscopy. The root-mean-square (RMS) roughness did not vary significantly with brush height (0.29 and 0.48 nm for brushes of lengths 12 and 30 nm, respectively, Fig. S13 in the ESI†), and thus differences in surface roughness were unlikely to cause the observed hysteretic memory behavior in contact angle. Similarly, comparison of Fig. 2(a) and (b) shows that hysteretic memory behavior in contact angle is not explained by variations in brush length: brushes with as-synthesized dry thicknesses of 12, 22, and 30 nm exhibited hysteretic pH-dependent contact angles, whereas their pH-responsive thicknesses were largely independent of the direction of pH change. Fig. 4 further supports this conclusion, as brushes with comparable lengths nonetheless exhibited vast differences in the degree of hysteretic memory behavior.

Next, we considered explanations related to brush kinetics. Earlier studies quantified the swelling and collapse kinetics of PAA brushes using QCM,<sup>58</sup> QCM with dissipation monitoring (QCM-D),<sup>65</sup> and surface plasmon resonance (SPR) spectroscopy.<sup>64</sup> Kurosawa *et al.* observed changes in frequency on the time scale of tens of minutes after switching brushes of molecular weights around 4 and 14 kg mol<sup>-1</sup> between pH 4.0, 4.8, and 5.4.<sup>58</sup> Liu and Zhang reported changes in the oscillation frequency as the pH was repeatedly cycled between 3.2 and 6.6, and the time over which the frequency changed was short compared to the 20 min time scale of the oscillation.<sup>65</sup> Finally, Sarkar and Somasundaran showed that the angular position of the reflectance dip of PAA, with molecular weight ranging from 50 to 3000 kg mol<sup>-1</sup>, changed over time scales of tens of seconds as the pH was repeatedly cycled between 3.5 and 9.5; swelling in these experiments took longer than collapse.<sup>64</sup> Although the response times reported in these studies vary widely, all time scales are shorter than the 30 minute equilibrium time used for our brush measurements. Moreover, we checked that the contact angle did not significantly change over time scales of longer than 30 minutes (Table S4 in the ESI†). We therefore concluded that the kinetics of swelling and deswelling likely did not play a role in the observed pH response of our PAA brushes.

We also considered the effect of substrate interactions on the pH-response of brushes of varying lengths.<sup>66</sup> We modeled the polymer brush as a PAA sphere (with surface area equal to  $\sigma^{-1}$ , 2.6 nm<sup>2</sup> per chain, and Hamaker constant reported for PAA in ref. 67,  $9.15 \times 10^{-21}$  J) separated from the silicon oxide substrate by a distance  $d$ . The van der Waals free energy, calculated as a function of  $d$ ,<sup>68</sup> decreased below  $kT$  a short distance from the substrate (around 0.2 nm). We therefore concluded that substrate interactions were unlikely to explain differences in the response of brushes of varying length, such as the low-pH contact angle and degree of swelling.

Instead, we suggest that the observed trends in the pH response of the brushes are governed by differences in brush dispersity. Milner and collaborators showed theoretically that

increased dispersity can increase the thickness of polyelectrolyte brushes.<sup>69</sup> de Vos and collaborators showed theoretically that increased dispersity can significantly change the volume fraction profile of the brush.<sup>70</sup> The three trends in the pH-responsive thickness and contact angle reported in this study could be explained by differences in the dispersity of the brushes examined here. (i) We suggest that the collapse of the brushes at low pH (Fig. 2(a)) is aided by conformational changes proposed by de Vos *et al.* for higher dispersity brushes, in which the longest chains near the brush surface are less extended than the chains near the substrate in densely grafted systems.<sup>70</sup> In support of this idea, the 12 nm brush had the lowest  $D$  of the brushes included in Fig. 2 (Table S1, ESI†), and exhibited the lowest percentage increase in dry thickness upon decreasing pH (Table 1). The 7 nm brush series with varying dispersity also exhibited a very low percentage increase in dry thickness upon decreasing pH (Table 2); we suggest that these low molecular weight chains have a reduced driving force for phase separation. (ii) We posit that the thickness of the collapsed layer near the brush surface at low pH increases with brush dispersity, resulting in the increase of the low pH contact angle (and degree of hydrophobicity) shown in Fig. 2(b) and 4(b). Comparison of the two higher dispersity brushes in Fig. 4, which exhibited similar low-pH contact angles, may indicate that there is a critical dispersity above which no further increase in the low-pH contact angle is observed. (iii) Finally, we suggest that the presence of this collapsed region at the brush surface prevents solvent and counterions from penetrating into the brush (as shown in the schematic mechanism in Fig. 6) and hence generates the hysteretic memory behavior in the contact angle observed in this study (Fig. 2–5). In particular, the 7 nm brush with the lowest dispersity in Fig. 4 showed no hysteretic memory behavior; moreover, across both series of experiments the degree of hysteretic memory behavior (quantified by  $\Delta pK_a$ , as shown in Fig. 5) increased with dispersity. Together, these results suggest that brush dispersity generates hysteretic memory and can serve as a design parameter to tune the responsive properties of polyelectrolyte brushes.

## Conclusion

We synthesized a series of poly(acrylic acid) brushes of varying length and dispersity and characterized changes in the dry thickness and static water contact angle as the pH was first decreased from 10 to 3 and then increased from 3 to 10. From these measurements, we report three trends in the pH-response: (i) the thickness of dry brushes increased upon increasing pH for brushes above a critical length; (ii) the low-pH contact angle increased with increasing dispersity; (iii) brushes of sufficient dispersity exhibited hysteretic memory behavior at intermediate pH; as a result, the  $pK_a$  measured upon increasing pH was greater than that upon decreasing pH. The degree of hysteretic memory behavior (as quantified by the difference in the  $pK_a$  values measured upon increasing and decreasing pH) increased with brush dispersity. To explain this response, we proposed a hypothetical physical picture in which solvent was excluded from the collapsed PAA brush at pH 3; as a result, the onset of swelling

was delayed to higher pH by the inability of the solvent to penetrate the brush. We posited that the trends observed in this study originate from differences in the dispersity of the brushes. This study systematically assesses the pH-response for PAA brushes of varying length and dispersity through careful synthesis and thorough characterization. Here we identify one unanticipated consequence of high brush dispersity, the hysteretic memory behavior, and show that its extent can be controlled using synthetic methods that modulate brush dispersity. These results have implications for applications in which polyelectrolyte brushes are repeatedly cycled (such as in self-cleaning surfaces) or in which the same material is used in different settings (for example, as antifouling coatings to remove both proteins and cells from surfaces, which may require different brush responses). All applications that leverage the abrupt changes in properties at the  $pK_a$  will benefit from knowledge of the effect of direction of pH change on the  $pK_a$ . Importantly, this study indicates that dispersity can be used as an additional design parameter to tune brush response. Finally, because the water contact angle is thought to probe the degree of dissociation of charges near the polyelectrolyte brush surface, we expect that brush dispersity may have other practical consequences for the response of pH brushes in a fully hydrated state; experiments to identify and probe these consequences are underway.

## Acknowledgements

We thank Gila Stein, Saeed Ahmadi Vaselabadi, and Abhijit Patil for access to and training on the ellipsometer, contact angle measuring instrument, and FTIR spectrometer. We thank Mahesh Mahanthappa for his insight into methods to modify the dispersity in ATRP syntheses, specifically his idea to use a reducing agent (e.g. phenylhydrazine). We thank Charles Anderson for access and training in the University of Houston Department of Chemistry Nuclear Magnetic Resonance Facility. We also thank Boris Makarenko and the University of Houston Department of Chemistry Characterization Facility for access to and training on the XPS spectrometer. We thank Peter Vekilov, Jeffrey Rimer, and Katy Olafson for access to and training on the atomic force microscope and Navin Varadarajan for access to the plasma cleaner. We thank Kim Mongcopa and Daehak Kim for helpful advice regarding the SI-ATRP process. Finally, we thank Ramanan Krishnamoorti and Richard Willson for insightful discussions. JCC acknowledges support from the National Science Foundation (DMR-1151133) and the Welch Foundation (E-1869). MLR acknowledges support from the National Science Foundation (CBET-1437831).

## References

- 1 P. M. Mendes, *Chem. Soc. Rev.*, 2008, **37**, 2512–2529.
- 2 D. Roy, J. N. Cambre and B. S. Sumerlin, *Prog. Polym. Sci.*, 2010, **35**, 278–301.
- 3 M. A. C. Stuart, W. T. S. Huck, J. Genzer, M. Muller, C. Ober, M. Stamm, G. B. Sukhorukov, I. Szleifer, V. V. Tsukruk, M. Urban, F. Winnik, S. Zauscher, I. Luzinov and S. Minko, *Nat. Mater.*, 2010, **9**, 101–113.
- 4 P. G. de Gennes, *Macromolecules*, 1980, **13**, 1069–1075.
- 5 K. R. Shull, *J. Chem. Phys.*, 1991, **94**, 5723–5738.
- 6 B. Lego, W. G. Skene and S. Giasson, *Macromolecules*, 2010, **43**, 4384–4393.
- 7 G. Sudre, D. Hourdet, C. Creton, F. Cousin and Y. Tran, *Macromol. Chem. Phys.*, 2013, **214**, 2882–2890.
- 8 M. K. Granfeldt, S. J. Miklavic, S. Marcelja and C. E. Woodward, *Macromolecules*, 1990, **23**, 4760–4768.
- 9 E. B. Zhulina, O. V. Borisov and V. A. Priamitsyn, *J. Colloid Interface Sci.*, 1990, **137**, 495–511.
- 10 O. V. Borisov, T. M. Birshtein and E. B. Zhulina, *J. Phys. II*, 1991, **1**, 521–526.
- 11 E. B. Zhulina, O. V. Borisov and T. M. Birshtein, *J. Phys. II*, 1992, **2**, 63–74.
- 12 H. Chen, R. Zajac and A. Chakrabarti, *J. Chem. Phys.*, 1996, **104**, 1579–1588.
- 13 C. Seidel, *Macromolecules*, 2003, **36**, 2536–2543.
- 14 R. Israels, F. A. M. Leermakers, G. J. Fleer and E. B. Zhulina, *Macromolecules*, 1994, **27**, 3249–3261.
- 15 Y. V. Lyatskaya, F. A. M. Leermakers, G. J. Fleer, E. B. Zhulina and T. M. Birshtein, *Macromolecules*, 1995, **28**, 3562–3569.
- 16 R. Nap, P. Gong and I. Szleifer, *J. Polym. Sci., Part B: Polym. Phys.*, 2006, **44**, 2638–2662.
- 17 K. Kurihara, T. Kunitake, N. Higashi and M. Niwa, *Langmuir*, 1992, **8**, 2087–2089.
- 18 R. Israëls, F. A. M. Leermakers and G. J. Fleer, *Macromolecules*, 1994, **27**, 3087–3093.
- 19 E. B. Zhulina, T. M. Birshtein and O. V. Borisov, *Macromolecules*, 1995, **28**, 1491–1499.
- 20 E. P. K. Currie, A. B. Sieval, M. Avena, H. Zuillhof, E. J. R. Sudhölter and M. A. Cohen Stuart, *Langmuir*, 1999, **15**, 7116–7118.
- 21 E. P. K. Currie, A. B. Sieval, G. J. Fleer and M. A. C. Stuart, *Langmuir*, 2000, **16**, 8324–8333.
- 22 P. Gong, J. Genzer and I. Szleifer, *Phys. Rev. Lett.*, 2007, **98**, 018302.
- 23 P. Gong, T. Wu, J. Genzer and I. Szleifer, *Macromolecules*, 2007, **40**, 8765–8773.
- 24 S. M. Kilbey II and J. F. Ankner, *Curr. Opin. Colloid Interface Sci.*, 2012, **17**, 83–89.
- 25 O. V. Borisov, E. B. Zhulina and T. M. Birshtein, *Macromolecules*, 1994, **27**, 4795–4803.
- 26 P. M. Biesheuvel, *J. Colloid Interface Sci.*, 2004, **275**, 97–106.
- 27 T. Wu, P. Gong, I. Szleifer, P. Vlček, V. Šubr and J. Genzer, *Macromolecules*, 2007, **40**, 8756–8764.
- 28 X. Wang, G. Liu and G. Zhang, *Langmuir*, 2011, **27**, 9895–9901.
- 29 S. R. Holmes-Farley, R. H. Reamey, T. J. McCarthy, J. Deutch and G. M. Whitesides, *Langmuir*, 1985, **1**, 725–740.
- 30 S. E. Creager and J. Clarke, *Langmuir*, 1994, **10**, 3675–3683.
- 31 N. Houbenov, S. Minko and M. Stamm, *Macromolecules*, 2003, **36**, 5897–5901.
- 32 K. Yu, H. Wang, L. Xue and Y. Han, *Langmuir*, 2007, **23**, 1443–1452.

- 33 R. Dong, M. Lindau and C. K. Ober, *Langmuir*, 2009, **25**, 4774–4779.
- 34 D. Aulich, O. Hoy, I. Luzinov, M. Brücher, R. Hergenröder, E. Bittrich, K.-J. Eichhorn, P. Uhlmann, M. Stamm, N. Esser and K. Hinrichs, *Langmuir*, 2010, **26**, 12926–12932.
- 35 Y. Lu, A. Zhuk, L. Xu, X. Liang, E. Kharlampieva and S. A. Sukhishvili, *Soft Matter*, 2013, **9**, 5464–5472.
- 36 R. Kumar, B. G. Sumpter and S. M. Kilbey II, *J. Chem. Phys.*, 2012, **136**, 234901.
- 37 G. J. Dunderdale, C. Urata and A. Hozumi, *Langmuir*, 2014, **30**, 13438–13446.
- 38 G. J. Dunderdale, C. Urata, D. F. Miranda and A. Hozumi, *ACS Appl. Mater. Interfaces*, 2014, **6**, 11864–11868.
- 39 G. J. Dunderdale, M. W. England, C. Urata and A. Hozumi, *ACS Appl. Mater. Interfaces*, 2015, **7**, 12220–12229.
- 40 C. Deodhar, E. Soto-Cantu, D. Uhrig, P. Bonnesen, B. S. Lokitz, J. F. Ankner and S. M. Kilbey II, *ACS Macro Lett.*, 2013, **2**, 398–402.
- 41 B. T. Cheesman, E. G. Smith, T. J. Murdoch, C. Guibert, G. B. Webber, S. Edmondson and E. J. Wanless, *Phys. Chem. Chem. Phys.*, 2013, **15**, 14502–14510.
- 42 J. D. Willott, T. J. Murdoch, B. A. Humphreys, S. Edmondson, G. B. Webber and E. J. Wanless, *Langmuir*, 2014, **30**, 1827–1836.
- 43 V. A. Pryamitsyn, F. A. M. Leermakers, G. J. Fleer and E. B. Zhulina, *Macromolecules*, 1996, **29**, 8260–8270.
- 44 M. G. Santonicola, G. W. de Groot, M. Memesa, A. Meszyńska and G. J. Vancso, *Langmuir*, 2010, **26**, 17513–17519.
- 45 N. Schüwer and H.-A. Klok, *Langmuir*, 2011, **27**, 4789–4796.
- 46 F. Xia, L. Feng, S. Wang, T. Sun, W. Song, W. Jiang and L. Jiang, *Adv. Mater.*, 2006, **18**, 432–436.
- 47 N. D. Treat, N. Ayres, S. G. Boyes and W. J. Brittain, *Macromolecules*, 2006, **39**, 26–29.
- 48 S. S. Balamurugan, B. Subramanian, J. G. Bolivar and R. L. McCarley, *Langmuir*, 2012, **28**, 14254–14260.
- 49 K. Matyjaszewski, W. Jakubowski, K. Min, W. Tang, J. Huang, W. A. Braunecker and N. V. Tsarevsky, *Proc. Natl. Acad. Sci. U. S. A.*, 2006, **103**, 15309–15314.
- 50 L. J. Kirwan, P. D. Fawell and W. van Bronswijk, *Langmuir*, 2003, **19**, 5802–5807.
- 51 S. Deng and Y. P. Ting, *Langmuir*, 2005, **21**, 5940–5948.
- 52 J. Dai, Z. Bao, L. Sun, S. U. Hong, G. L. Baker and M. L. Bruening, *Langmuir*, 2006, **22**, 4274–4281.
- 53 H.-Y. Yu, Z.-K. Xu, Q. Yang, M.-X. Hu and S.-Y. Wang, *J. Membr. Sci.*, 2006, **281**, 658–665.
- 54 M. Suchoparek and J. Spevacek, *Macromolecules*, 1993, **26**, 102–106.
- 55 W. Liu, T. Nakano and Y. Okamoto, *Polym. J.*, 1999, **31**, 479–481.
- 56 S. Venkataraman and K. L. Wooley, *Macromolecules*, 2006, **39**, 9661–9664.
- 57 G. Li, S. Song, L. Guo and S. Ma, *J. Polym. Sci., Part A: Polym. Chem.*, 2008, **46**, 5028–5035.
- 58 S. Kurosawa, H. Aizawa, Z. A. Talib, B. Atthoff and J. Hilborn, *Biosens. Bioelectron.*, 2004, **20**, 1165–1176.
- 59 N. Ayres, S. G. Boyes and W. J. Brittain, *Langmuir*, 2007, **23**, 182–189.
- 60 G. Sudre, E. Siband, D. Hourdet, C. Creton, F. Cousin and Y. Tran, *Macromol. Chem. Phys.*, 2012, **213**, 293–300.
- 61 A. Zengin, G. Karakose and T. Caykara, *Eur. Polym. J.*, 2013, **49**, 3350–3358.
- 62 D. Aureau, F. Ozanam, P. Allongue and J.-N. Chazalvier, *Langmuir*, 2008, **24**, 9440–9448.
- 63 F. A. Plamper, H. Becker, M. Lanzendörfer, M. Patel, A. Wittemann, M. Ballauff and A. H. E. Müller, *Macromol. Chem. Phys.*, 2005, **206**, 1813–1825.
- 64 D. Sarkar and P. Somasundaran, *Langmuir*, 2004, **20**, 4657–4664.
- 65 G. Liu and G. Zhang, *J. Phys. Chem. B*, 2008, **112**, 10137–10141.
- 66 S. M. Sirard, R. R. Gupta, T. P. Russell, J. J. Watkins, P. F. Green and K. P. Johnston, *Macromolecules*, 2003, **36**, 3365–3373.
- 67 K. Feldman, T. Tervoort, P. Smith and N. D. Spencer, *Langmuir*, 1998, **14**, 372–378.
- 68 J. N. Israelachvili, *Intermolecular and Surface Forces*, Academic Press, London, 2nd edn, 1991.
- 69 S. T. Milner, T. A. Witten and M. E. Cates, *Macromolecules*, 1989, **22**, 853–861.
- 70 W. M. de Vos and F. A. M. Leermakers, *Polymer*, 2009, **50**, 305–316.